

CHAPTER IV

PHOTOELECTROCHEMICAL CELL HYDROGEN PRODUCTION

The photodecomposition of water at the some surface semiconductor surface requires that the difference between the redox potential of electrons and holes exceed the decomposition voltage of water, as explained in Chapter III. But this is not sufficient since each of the individual redox reactions of electrons and holes must have the necessary driving force. This condition is fulfilled if the Fermi level of electron is above the Fermi level of the water/hydrogen redox system and the Fermi level of holes below the Fermi energy of the oxygen/water redox system. Therefore the combination of n and p-type semiconductors were used in the photoelectrochemical cells (PEC'S). The band edges of semiconductors in relation to the electrolyte have to be located in such a range of energies that at each electrode one of the reactions can be performed by the minority carriers if the surface is illuminated. The principles of such a system are explained in Figure 4. The disadvantages of all systems where two semiconductor electrodes with opposite photovoltages are used in one electrolytic all suffer from the difficulty that the photogenerated currents have to be well balanced in order to avoid additional losses since the current output of the all must be balanced and the less efficient electrode will take over control.

Up to now, there are many ways for the development of PEC'S, used for hydrogen synthesis from water such as pH bias, increasing light absorption

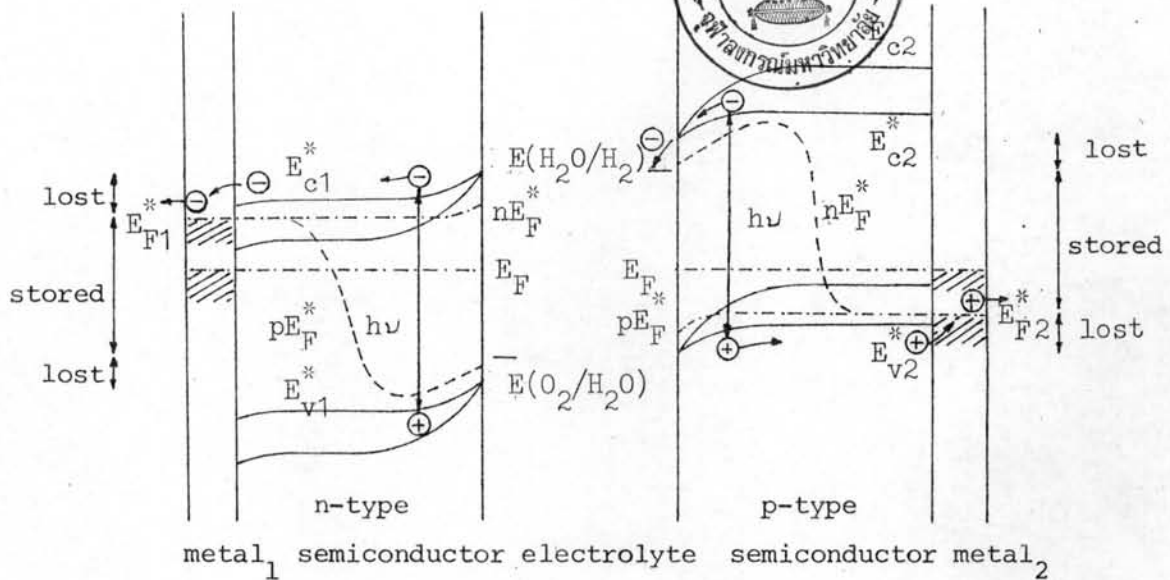


Figure 4 Energy correlations in photoelectrolytic cell for water decomposition with two illuminated semiconductor electrodes (n-type and p-type) generating photovoltages of opposite sign. (11)

of photoelectrodes by doping impurity. All systems will be discussed in this chapter.

4.1 Energy Requirements for Photoelectrolysis of Water

4.1.1 Cell Potential for Electrolysis

In electrolysis, only the free energy of reaction, ΔG , can be interchanged with electrical energy at constant temperature and pressure. The quantity of electric charge corresponding to the molar quantities indicated in the balanced chemical equation is nF , where n is the number of electrons transferred per molecule and F is the Faraday value.

If this quantity of electrical charge is transported through a potential difference of E volts, the amount of work required is given by nFE .

Because this electrical change does not involve pressure-volume work and is carried out isothermally, the change in Gibbs free energy is given by

$$\Delta G = -nFE \quad \dots 4.1.1$$

where E is the potential difference, or voltage.

The entropy change for an electrolytic-cell reaction may be calculated from the temperature coefficient of the electromotive force because

$$\left(\frac{\partial \Delta G}{\partial T} \right)_P = \Delta S$$

Introducing this into 4.1.1 gives

$$nF \left(\frac{\partial E}{\partial T} \right)_P = \Delta S \quad \dots 4.1.2$$

The enthalpy change for the cell reaction may be calculated by substituting Eq. 4.1.1 and 4.1.2 into

$$\Delta H = \Delta G + T\Delta S = -nFE + nFT \left(\frac{\partial E}{\partial T} \right)_P \quad \dots 4.1.3$$

It is apparent from Eq 4.1.3 that this difference between the free energy change and the total energy change (enthalpy) is accounted for by an entropy change in the process. Because the entropy change cannot be converted to electricity, it must be supplied or liberated as heat.

For a water electrolysis cell, it can be calculated that the voltage corresponding to the enthalpy change, to the heat of combustion of hydrogen, is 1.47 volts at 25°C, whereas the cell voltage corresponding to the free-energy change is only 1.23 volt.

In an ideal case, then 1.47 volts applied to a water electrolysis cell at 25^oc would generate hydrogen and oxygen isothermally, that is, at 100 % thermal efficiency with no waste heat produced. However, a voltage as low as 1.23 volts would still generate hydrogen and oxygen, but the cell would absorb heat from its surroundings. The electrical energy required for the process is only 83.7 % of the combustion energy of hydrogen produced; the other 16.3 % is supplied as heat.

In practical cells, there is usually an efficiency loss that is greater than the difference between the free energy voltage and the enthalpy voltage. In other words, practical cells usually operate at voltages greater than 1.47 volts and liberate heat because of a variety of efficiency loss occurring with the cell. The heat required to supply the entropy of reaction is therefore provided by some of this waste heat, and practical cells do not absorb heat from their surroundings. Therefore the cell potential, E , or the free-energy change voltage varies with temperature as shown in Figure 4.1.1. As can be run, raising the temperature lower the voltage at which water can be decomposed. This factor operates in favor of electrolysis cells because at higher temperatures the electrode processes proceed faster, with less loss, while the required energy input is less.

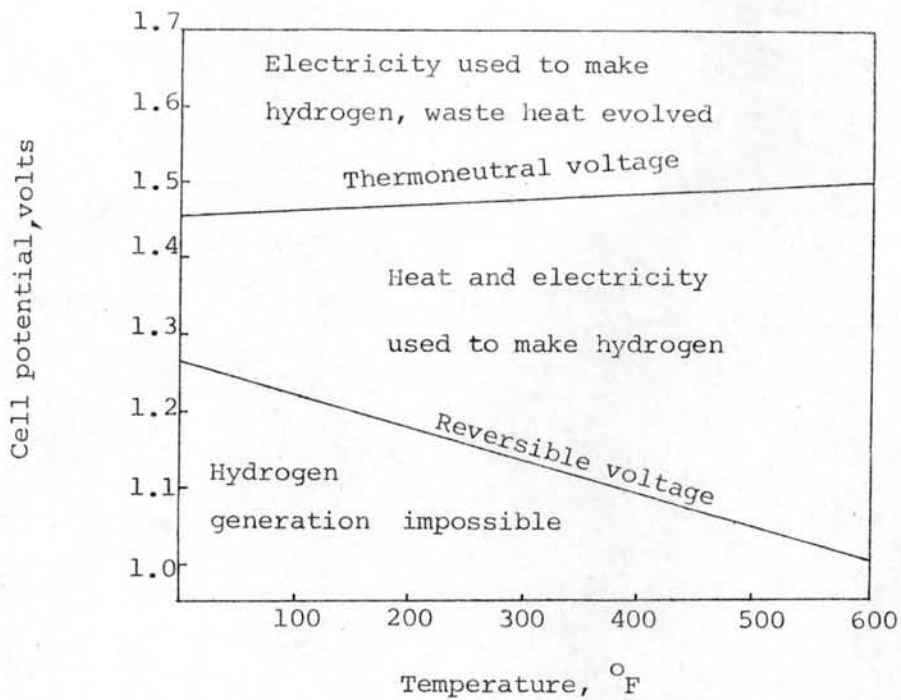


Figure 4.1.1 Idealized operating conditions for electrolyzer. ⁽¹⁶⁾

Three areas, therefore can be identified:

- i) that in which no hydrogen is evolved,
- ii) that in which hydrogen is made at an apparently greater-than-100 % efficiency and
- iii) that in which hydrogen is made at an efficiency of less than 100 % with the production of waste heat.

The voltage corresponding to enthalpy change, or the thermoneutral voltage, varies only slightly with temperature, from 1.47 V at 25°C to 1.50 V at 340°C.

In order to study the effect of pressure on electrolysis, the free energy change can be written as

$$\Delta G = -SdT + VdP \quad \dots 4.1.4$$

If this is applied at constant temperature Eq. 4.1.4 can be written

$$\frac{\partial G}{\partial P}_P - \frac{\partial G}{\partial P}_R = V_P - V_R$$

where G_r , G_p , V_r , and V_p are the Gibbs free energy and volume of the reactants and product, respectively. This equation may be written

$$\frac{\partial G_p}{\partial P} - \frac{\partial G_r}{\partial P} = V_p - V_r$$

where G_r , G_p , V_r , and V_p are the Gibbs free energy and volume of the reactants and product, respectively. This equation may be written

$$\frac{\partial \Delta G}{\partial P} = \Delta V \quad \dots 4.1.5$$

where ΔV is the change in volume during reaction. Substituting ΔG into Eq. 4.1.5, therefore

$$\frac{\partial E}{\partial P} = \frac{-\Delta V}{nF}$$

Assuming that the volume of the liquid water is small compared with that of gaseous products hydrogen (H_2) and oxygen (O_2) and further assuming the volumes of these gases obey the perfect gas law

$$PV = ZRT$$

where Z = number of moles, therefore

$$dE = \left(\frac{ZRT}{nF} \cdot \frac{dP}{P} \right)_{O_2} + \left(\frac{ZRT}{nF} \cdot \frac{dP}{P} \right)_{O_2}$$

By integration between ambient conditions and the operating pressure ⁽¹⁶⁾

$$E_p = E_1 + \frac{0.052}{2} \log P_{H_2} + \frac{0.058}{4} \log P_{O_2}$$

For $P_{H_2} = P_{O_2}$ during electrolysis

$$E_p = E_1 + 0.0435 \log P \quad (P \text{ in atm}) \quad \dots 4.1.6$$

This, raising the pressure of operation of a water electrolyzer results in a theoretical increase in the decomposition voltage of 43 mV for every tenfold increase in pressure.

However, for water electrolysis to be competitive with the conventional methods of hydrogen production, it is necessary to operate the electrolysis cells at the highest current densities and at voltages as close as possible to the thermoneutral potential (Figure 4.1.1). But in practical cells, there are some parameters to be discussed. For cell potential, E_{cell} may be represented by an equation of the form

$$E_{cell} = E_r + \eta_a + \eta_c + iR \quad \dots 4.1.7$$

where E_r is the thermodynamic reversible potential for the cell, 1.23 eV, η_a and η_c are anodic and cathodic over voltages and may be expressed as a function of the current density, i , by the Tafel equation⁽⁹⁾ of the form

$$\eta = a + b \log i \quad \dots 4.1.8$$

where a and b are constants which yield information on the electrocatalytic activities and the mechanism of the hydrogen and oxygen electrode reactions. iR is the ohmic drop in the electrolyte.

There are some methods of improving the efficiency of a water electrolysis cell. They are⁽¹⁶⁾

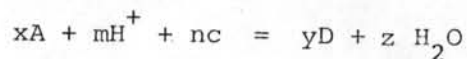
i) maximization of real to apparent surface area of electrode to reduce activation overpotential,

ii) increase of operating temperature to reduce activation and ohmic overpotential losses, and

iii) reduction of the thickness between electrodes to decrease the ohmic drop in the cell.

4.1.2 The pH-potential diagram

Bockris and Reddy⁽⁹⁾ have explained the pH-potential diagram of water decomposition by electrolysis. In predicting the equilibrium potential difference across cells, at both electrode-electrolyte inter-faces, they proposed the reaction



Then the Nernst equation assumed the form

$$E = E^{\circ} + \frac{RT}{nF} \ln(a_A^x \cdot a_H^m / a_D^y \cdot a_{H_2O}^z)$$

For the activity of water, a_{H_2O} , equals unity, then

$$E = E^{\circ} + \frac{2.303RT}{nF} \log(a_A^x / a_D^y) + \frac{2.303}{nF} \log a_H^m$$

But there is a convenient scale for expressing the activity of hydrogen ions, a_H^m in a solution, the pH scale

$$pH = -\log a_H^m$$

therefore

$$E = E^{\circ} + \frac{2.303RT}{nF} \log \frac{a_A^x}{a_D^y} - \frac{2.303RT}{F} \frac{m}{n} pH \quad \dots 4.1.9$$

Consider the reaction



By experimental data, Eq.4.1.9 will give a straight line with a slope of $(-2.303RT/F) \cdot \frac{m}{n}$ by plotting the electrode potential against pH.

They found the parameters of Eq.4.1.10, $x = 1$, $A = O_2$, $m = 4$, $n = 4$, and $y = 0$. Thus,

$$E = E^{\circ} + \frac{2.303RT}{4F} \log P_{O_2} - \frac{2.303RT}{F} \text{pH}$$

where P_{O_2} is the partial pressure of O_2 gas. If this is taken as 1 atm and the numerical value of RT/F at 25°C is inserted, then

$$E = E^{\circ} - 0.059 \text{ pH}$$

From Table A.3, $E^{\circ} = 1.23 \text{ V}$ and, hence

$$E = 1.23 - 0.059 \text{ pH} \quad \dots 4.1.11$$

Similar considerations shows that the equilibrium potential of hydrogen electrode is pH dependent since the Nernst equation for the reaction



is

$$E = E^{\circ} + \frac{2.303RT}{2F} \log P_{\text{H}_2} - \frac{2.303RT}{F} \text{pH}$$

and, for $P_{\text{H}_2} = 1$ at 25°C

$$E = -0.059 \text{ pH} \quad \dots 4.1.13$$

A simple pictorial pH versus potential presentation can be used for the equilibrium situation in an oxygenhydrogen cell (Figure 4.1.2). Although the potentials of both electrodes are pH dependent, the cell potential (represented by the distance of the points of intersection of a perpendicular erected at any desired pH, is 1.23 for water decomposition by electrolysis) remains constant since both electrode potentials change in the same way with varying pH.

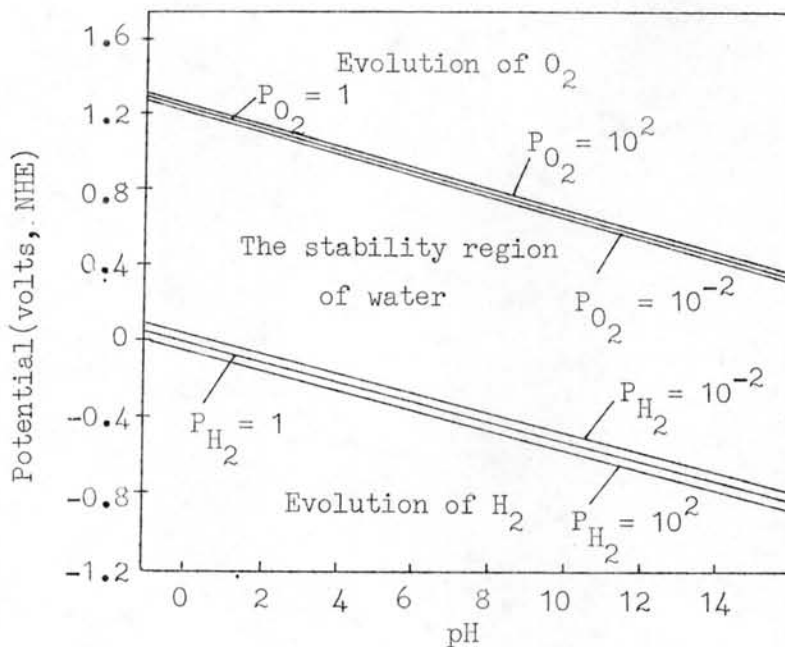


Figure 4.1.2 The equilibrium potential difference of an oxygen-hydrogen cell does not depend on the pH and can be obtained at any pH as a difference between the two lines.

4.1.3 Photoelectrolysis of Water

Photoelectrolysis of water by a photoelectrochemical cell is demonstrated in Chapter III, the exact energy required for this purpose should be greater than the theoretical free energy (1.23 eV). For a Schottky barrier device with a counterelectrode for photoelectrochemical cell as shown in Figure 4.1.3. The necessity

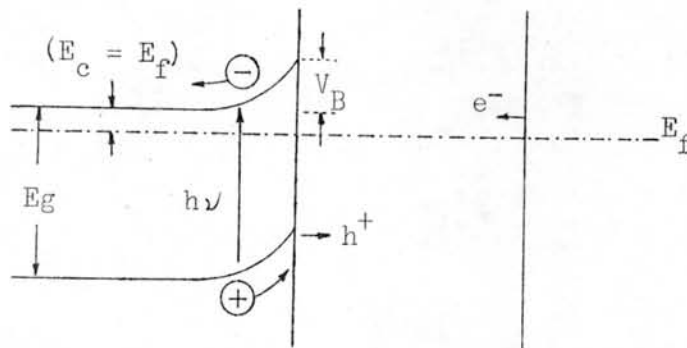


Figure 4.1.3 Energy relationships for an illuminated semiconductor electrode in contact with a solution

for bias to produce gaseous evolution can be understood by considering an energy balance for the absorbed photon of light. For band-gap photon ($h\nu \geq E_g$): (58,74)

$$E_g + V_A = V_B + (E_c - E_f) + \frac{\Delta G}{nF} + \eta_a + \eta_c + iR + V_H \dots 4.1.14$$

where E_g is the semiconductor bandgap, V_A is any applied external bias, V_B is the potential barrier of the semiconductor electrolyte junction, E_c is the conduction band energy, E_f is the Fermi level at equilibrium, $\Delta G/nF$ is the free energy change per electron for the chemical reaction, η_a and η_c are the respective over-potential at the anode and cathode, iR is the ohmic loss, and V_H is the potential drop across the Helmholtz layer in the electrolyte (see 3.3.2). For chemical energy stored by this system, so the parameters in Eq 3.1.14 will be considered. Nozik⁽⁷⁴⁾ considered the energy balance in a photoelectrolysis cell with TiO_2 electrode as anode, and he estimated the values of energy requirements for gaseous (H_2, O_2) evolution, 3.3-3.5 eV of input energy. Therefore, this is the reason for the water decomposition in photoelectrochemical cells, wide band-gap Semiconductors (e.g. $TiO_2, SrTiO_3$) should be always used as the photoelectrode, and as a consequence, the short wavelength light (ultraviolet) will be required for this system. Thus the conversion efficiency of solar energy to chemical energy will be reduced (see Fig 4.1.4)

4.1.4 Energy Conversion of Photocells

The maximum quantum efficiency depends on the threshold for absorption which is the optical energy gap E_g of semiconductor. It is represented by η_E , from Eq.2.1.2c, and is also the theoretical efficiency of photovoltaic devices. If the cell operates not as an energy source with optimal adjustment for power generation, but as a storage device, the efficiency is reached. Botton⁽¹⁰⁾ approximated this by the relation.

$$\eta_{\text{storage}} = \frac{E_{\text{storage}}}{E_g} \cdot \eta_E$$

Using this relation he obtained the range of optimal efficiency for energy storage by water decomposition as shown in Figure 4.1.4 as a function of the band gap. The real efficiency will be even lower due to reflection loss, unfavorable load adjustment and imperfections of barrier layer.

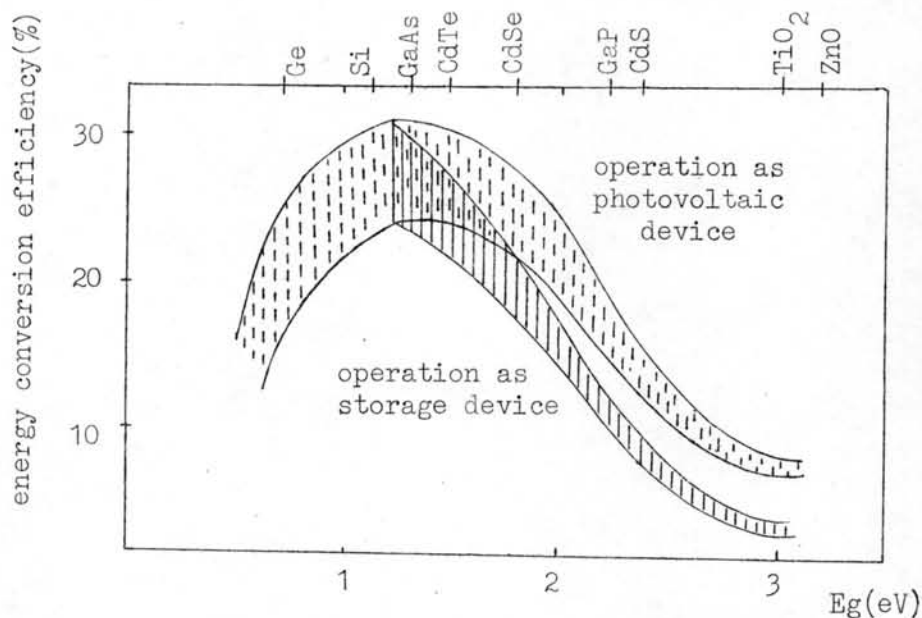


Figure 4.1.4 Theoretically predicted optimal efficiencies for solar energy conversion (AM1) by semiconductor photocells as photovoltaic power source⁽¹¹⁾

or a storage device by electrolytic water decomposition.

In practical cells there are a number of different ways to define the optical conversion efficiency of a photoelectrochemical cell. The yield of energy conversion to chemical energy is calculated according to the formular:⁽²⁾

$$\begin{aligned} \text{Incident energy conversion percent} \\ = \frac{(\text{chemically stored energy}) \times 100}{\text{energy input}} \end{aligned}$$

and

$$\begin{aligned} \text{Absorbed energy conversion percent} \\ = \frac{(\text{chemically stored energy}) \times 100}{\text{absorbed energy}} \quad \dots 4.1.15 \end{aligned}$$

where

$$\begin{aligned} \text{Chemically stored energy} &= (\text{Free energy of reaction per mole}) \times \\ &\quad \text{number of moles.} \end{aligned}$$

$$\begin{aligned} \text{Absorbed energy} &= \text{Energy flux} \times \text{irradiated surface} \times \\ &\quad \text{time} \times \text{absorbance percent} \end{aligned}$$

$$\begin{aligned} \text{Energy Input} &= \text{Energy flux} \times \text{irradiated surface} \times \text{time} \end{aligned}$$

and

$$\begin{aligned} \text{Absorbance percent} \\ = \frac{(\text{Incident energy flux} - \text{Transmitted energy flux}) (\text{percent energy} > \text{band gap})}{\text{Incident energy flux}} \end{aligned}$$

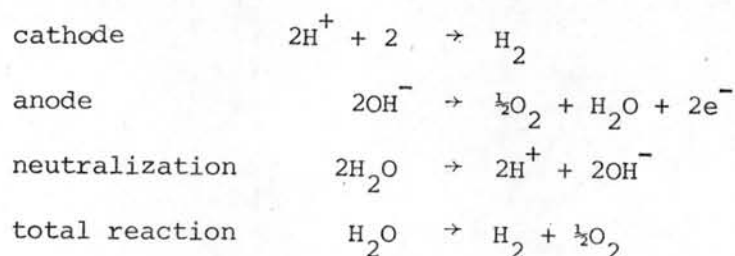
The simplest and most popular definition has been⁽³⁶⁾

$$\eta_1 = \frac{\text{energy output}}{\text{energy input}} \quad \dots 4.1.16$$

when the energy output is taken as the heat of combustion (ΔH) of the products. For hydrogen, formic acid, formaldehyde, methanol and

methane are 286, 270, 563, 727 and 890 KJ per mole respectively. The energy input is the intensity of the light source (lamp or sun). Not only sunlight conversion efficiency but also efficiency based on various solar simulator lamps (such as a xenon lamp but such sources do not have the same spectral content as sunlight and therefore do not allow comparison to be made.

For a photoelectrochemical cell is being biased by, maintaining different pH's in the anode and cathode compartment (see 4.2) then the heat of neutralization of H^+ by OH^- ought to be considered in the efficiency calculation. The cell reactions are



Thus, two charges are transferred through the circuit per mole of hydrogen produced. The heat of combustion of 1 mole of hydrogen is 68 kcal, which the heat of neutralization of 2 moles of H^+ is 28 kcal. Ghosh and Maruska⁽³⁶⁾ (1977) defined

$$\eta_2 = \frac{(I/nF).(68,000-28,000)}{I_a} \quad \dots 4.1.17$$

where I is the cell current ($mA.cm^{-2}$), $n = 2$, $F = 23,050$ C-cal/J.mole, and I_a is the energy constant of the incident light ($mW.cm^{-2}$)

For photoelectrochemical cell which has been biased by external energy (from power supply or solar cell), the energy conversion efficiency of radiant energy into chemical energy was calculated according to the following formula: (42,92)

$$\eta_3 = I \left[\left(\frac{\Delta H}{z} \right) - V_b \right] / I_a \quad \dots 4.1.18$$

where

I is the current flowing in the system, mA.cm^{-2} .

V_b is the electrical bias on the semiconductor electrodes.

ΔH is the heat of combustion of a product

z is the number of electrons required in the reduction of one molecule of H_2O or CO_2 to a molecule of product. They are 2, 2, 4 and 6 for production of hydrogen, formic acid, formaldehyde and methane.

Furthermore, it is possible to calculate the efficiency on the basis of free energies involved. If the hydrogen produced is to be used in a fuel cell, then it will generate a potential of 1.23 volts. The cell bias is now supplied by a variable voltage source, V_b , so that ⁽³⁶⁾

$$\eta_4 = \frac{I(1.23 - V_b)}{I_a} \quad \dots 4.1.19$$

This efficiency is strongly dependent on the magnitude of the bias voltage. Therefore, for a photocell without bias ($V_b = 0$) the efficiency is

$$\eta_5 = \frac{1.23I}{I_a} \quad \dots 4.1.20$$

4.2 Titanium Dioxide Electrode in Photocells

The natural forms of titanium dioxide, TiO_2 , are anatase, brookite and rutile. Rutile is the stable form of TiO_2 crystal. Some physical properties of TiO_2 crystal at room temperature are summarized as follows: ^(19,96)

molecular weight	79.9
Molecules/cm ³	3.18X10 ²²
density ρ (g/cm ³)	4.22
Energy gap(eV)	3.00
Mobility of electrons (cm ² /Vsec)	1

According to energy input for a photoelectrochemical cell up to 3 eV (see 4.1.3), TiO₂ used as the photoelectrode must be required bias for this system, such as biased by external power or solar cells. A interesting system for the all there are two compartments which are connected to one another through a bridge (Figure 5.2), one contains acidic solution and in which counterelectrode (Pt) is immersed, the other contains alkaline solution and in which TiO₂ is immersed. Therefore, this system is biased

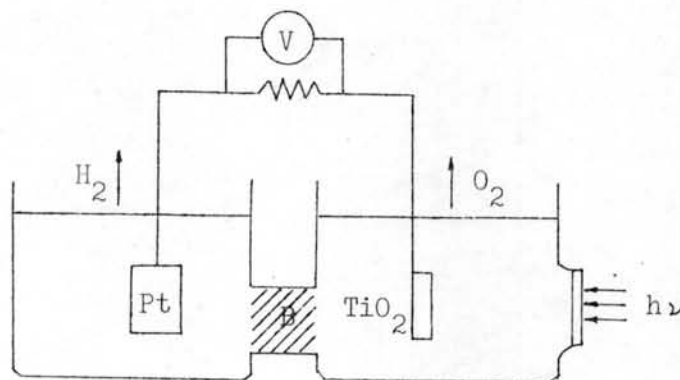
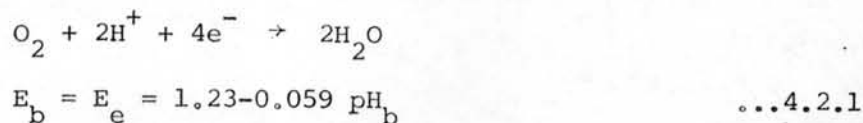


Figure 4.2 Photoelectrochemical cell or photoelectrolytic cell in which the TiO₂ electrode is connected with a platinum electrode. B is a salt bridge.

by the pH of solutions. For example, water electrolysis given pH_a for acidic solution and pH_b for alkaline solution, then the different of pH, ΔpH , of two compartment is

$$\Delta\text{pH} = \text{pH}_b - \text{pH}_a$$

Consider the water oxidation by Eq.5.1.10 and the equilibrium potential, $E_b = E_e$, in Eq.4.1.11 to be required for alkaline compartment,



Also, the reduction in the acidic compartment by Eq.4.1.12 and the equilibrium potential is shown as follows



Therefore, for water electrolysis in this system, the equilibrium potential required is

$$\begin{aligned} E_{\text{cell}} &= 1.23 - 0.059 \text{pH}_b - (-0.059 \text{pH}_a) \\ &= 1.23 - 0.059 \Delta\text{pH} \quad \dots 4.2.3 \end{aligned}$$

Thus, the potential bias in this cell is 0.059 Volts per ΔpH .

For only one compartment for a cell, water electrolysis in acidic solution ($\text{pH} < 7$) or alkaline solution ($\text{pH} > 7$) must always require a potential of 1.23 volts (see Figure 4.1.2).

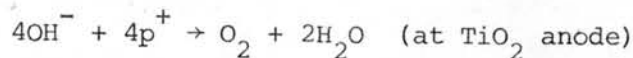
It is possible to use TiO_2 electrodes in photocells for hydrogen production, and this has been demonstrated by many investigators since 1972. (31, 34, 74) A suitable concentration of acidic and alkaline solution for a pH biased photocell was studied by Fujishima, (31, 34) 0.5 M H_2SO_4 for the acidic solution and 1M NaOH for the alkaline solution is the best system for hydrogen production by the photocell. And the liquid junction potential was actually lower than 0.05 Volts since a salt bridge consisting of agar

containing saturated KCl was used.

For TiO_2 as photoelectrodes, their forms are single crystal and polycrystal TiO_2 electrodes. The latter form is developed to form any thin film electrodes, such as by simple heating Ti-metal, the chemical vapor deposition. The use of thin film polycrystal TiO_2 in place of its single crystal is desired from the practical standpoint of realizing a large scale for the photocells, and sometimes it may be made a low cost electrode.

4.2.1 TiO_2 Single Crystal Electrodes.

Up to now, there are two systems for water photoelectrolysis by photocells. They are the photocell with one solution compartment, contained acidic or alkaline solution, and the other with two solution compartments for acidic and alkaline solution, as discussed above. The first time, water photocell demonstrated by Fujishima and Honda⁽³¹⁾ is the latter system, oxygen was evolved at the anode (TiO_2) and hydrogen at cathode (Pt) (Figure 4.2), the reactions in their electrolyte postulated as Eq.2.2.1, is the same as reactions for water photoelectrolysis with two half reactions (Eq.4.1.10 and 4.1.12) in the acidic solution, as electrolyte for a photocell with one compartment. In contrast to that, the alkaline solution, discussed by Wrighton et al.⁽¹⁷⁾, the hydrogen and oxygen reactions in photocell are:



the overall reaction



In the dark, $E_{\text{OH}^-/\text{O}_2}$ and $E_{\text{H}_2/\text{H}_2\text{O}}$ are + 0.40 V and -0.83 V (from Table A.3), then, the potential difference of this cell is still 1.23 V. For water photoelectrolysis in 5 M KOH, the potential of $E_{\text{OH}^-/\text{O}_2}$ is + 0.16 V vs. SCE and $E_{\text{H}_2/\text{H}_2\text{O}}$ is - 1.07 V vs. SCE, as shown in Fig 3.5.5 or 3.5.6.

The I-V characteristic for TiO_2 electrode in acidic electrolyte (pH 4.7) is shown in Figure 4.2.1, the $E_{\text{O}_2/\text{H}_2\text{O}}$ and $E_{\text{H}_2/\text{H}_2\text{O}}$ shift by 0.059 pH of Eq 4.2.1 and 4.2.2, then $E_{\text{O}_2/\text{H}_2\text{O}}$ and $E_{\text{H}_2/\text{H}_2\text{O}}$ are about -0.71V and + 0.52V v.s. SCE.

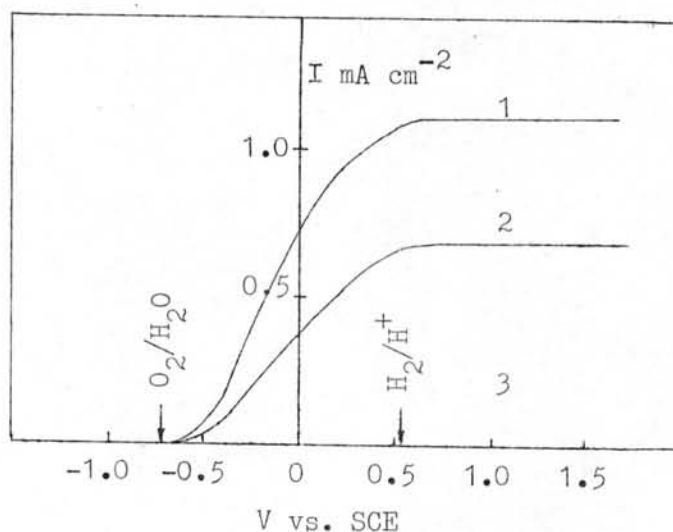


Figure 4.2.1 The I-V characteristic of TiO_2 single crystal semiconductor in the dark and illumination. (31)

1. high intensity
2. low intensity
3. in the dark.

Therefore, the I-V characteristic studies of TiO_2 electrode, the redox potentials in any solution and light intensities must be carefully considered. The I-V measurement by Harris and Wilson, (47) the circuit in Figure 4.2.2 was used to measure the voltampere relations of the two

half-cells or the photoresponse of the anode half-cell, and the polarities of the voltages and currents are defined there, the result was shown as likely the curve in Figure 4.2.1

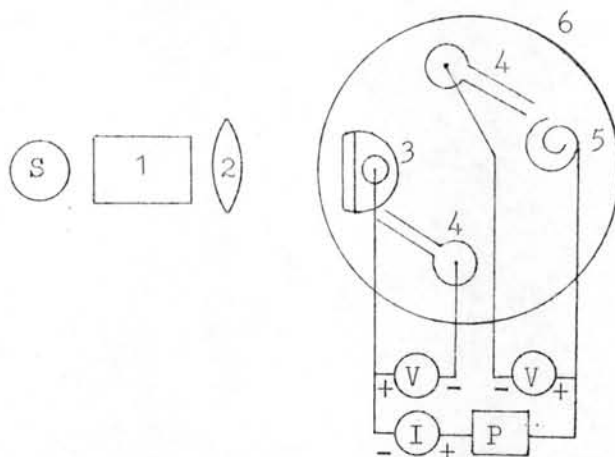


Figure 4.2.2 Schematic of experimental arrangement for photocurrent measurements. (47)

S, source, P, power supply

v, voltmeter, I, ammeter

1, monochromator, 2, quartz lenses

3, exposed face TiO_2 anode

4, luggin capillary, 5, platinum, 6, vycor beaker

From a I-V characteristic of TiO_2 photoelectrode, the starting potential of oxidation reaction ($\text{O}_2/\text{H}_2\text{O}$) indicates a ability of the electrode used for water photoelectrolysis, e.g. It is more negative than $E_{\text{H}_2/\text{H}_2\text{O}}$, ~ 1.03 V vs SCE in 5M KOH (Fig.4.5.5 and 4.5.6) and ~ 0.7 V vs SCE in solution of pH 4.7 Therefore, TiO_2 must be required for water decomposition with illumination, the minimum bias is 0.15-0.25 V. (60) However, there are TiO_2 electrodes used for water photoelectrolysis in photocell without bias.



doping TiO_2 electrodes with impurities (see 4.8.3). Another electrode parameters in photocells must be studied for the cell, they are quantum efficiency (see 3.5.2.), hole diffusion length, barrier width and the donor concentration.

The light response and quantum efficiency of TiO_2 single crystal were demonstrated by many investigators^(36,98) Under illumination of short wavelength (300-400 nm) one has a good response for the TiO_2 electrode^(36,58) (Figure 5.3.4). From computer program studies and variety of combinations of barrier widths and diffusion lengths for the photocurrent current Eq. 3.5.1a⁽³⁶⁾ The modified equation was used for this task by Salvador,⁽⁸²⁰⁾ from Eq 3.5.1c. and rearranged as follow:

$$\ln(1-\phi) = \alpha \left(\frac{\epsilon\epsilon_0}{2qN_D} \right)^{1/2} (V-V_{fb})^{1/2} - \ln(1-\alpha L_p)$$

where ϕ is the J/qNG term. This equation shows that a plot of $\ln(1-\phi)$ v.s. $(V-V_{fb})^{1/2}$ should be linear with an intercept on the ordinates axis of $-\ln(1+\alpha L_p)$, and with a slope of $-\alpha(\epsilon\epsilon_0/2qN_D)^{1/2}$. The longer hole diffusion length give a better response and conversion efficiency (see.4.2.3)

The donor concentrations are also obtained from capacitance measurements, when the semiconductor in contact with an aqueous electrolyte is in the depletion mode, by Eq.3.3.2b,

$$C_{sc}^{-2} = \frac{2}{q\epsilon\epsilon_0 N_D} (V-V_{fb} - kT/q)$$

The studies were demonstrated for calculation values of N_D and V_{fb} of photoelectrodes. (46, 87, 95)

For TiO_2 single crystals, the carrier or donor concentrations determined from the C_{sc} -V data were consistently in the 10^{20} cm^{-3} range,

and the barrier width in the 10^{-6} m range. (36, 58)

The electrode preparation is a important step of semiconductor, polishing and etching of TiO_2 electrodes were examined. (87, 95) Also, TiO_2 , was reduced in H_2 to produce an n-type conductivity. (74)

The efficiencies of photocell with TiO_2 photoanode for hydrogen production are discussed in 4.1.4. TiO_2 crystal in photocells with and without bias, their conversion efficiencies were in Table 4.2.1 (36)

Table 4.2.1a Conversion efficiencies of photocells with TiO_2 and Al doped TiO_2 photoanode in sunlight.

Biased system by	Efficiency (%)		η
	undoped TiO_2	Al doped TiO_2	
no bias	0.4	1.3	η_1 , Eq.4.1.16
pH bias	0.28	0.8	η_2 , Eq.4.1.17
bias of 0.4V	-	0.6	η_4 , Eq.4.1.19

The photocells biased by external power, Ghosh and Maruska (36) demonstrated the maximum efficiency is strongly dependent on the magnitude of bias voltage, their experiment the voltage was 0.4 volts in an Al-doped TiO_2 cell.

In 1980, Vandergesst and Fahidy (93) chose Al-doped TiO_2 and SrTiO_3 (95) as anode electrodes in photocells for solar water electrolysis plant. They studied the simulation of a hydrogen producing plant consisting of photocells decribed on the basis of mathematical modeling.

An interesting investigation is the demonstration of hydrogen synthesis by water photodecomposition in a photocell without any bias (e.g. pH bias, external power), so called a self-driving photocell, and the cell

will be a simple system, only one compartment with acidic or alkaline solution.

A p-n photoelectrolysis cell, consisting of an external source, These cells have nTiO₂-pGaP cell⁽¹⁷⁾, nSrTiO₃-pGaP cell and nSrTiO₃-pCdTe, etc. were tested by Ohashi,⁽⁷⁶⁾ showed the steady curve of these cell voltages in 1 M NaOH for 10 hours under xenon illumination. The efficiencies of cells was 0.04-0.7 % (by Eq.4.1.20).

A nFe₂O₃-pGaP cell was investigated by Metter et al.⁽⁶⁴⁾ in 1981. This cell splits water molecules using visible light with a low quantum efficiency. Surface catalysts of doping RuO₂ on nFe₂O₃ and Pt on pGaP can enhance the observed photocurrent, but the former are only temporarily. This cell also splits seawater using incident solar radiation

Another TiO₂ forms, Guruswamy and Bockris⁽⁴⁰⁾ coated lanthanum and chromium oxides on a TiO₃ single crystal. The electrodes were made by firing lanthanum and chromium oxides, or salts which are converted upon heating to the oxide, in a paste of citric acid on a titanium oxide base. The photocurrents obtained were around four times greater than on an TiO₂ single crystal in the some potential region. The efficiencies of conversion of solar light at LaCrO₃-TiO₂ (lanthanum chromite-titanate dioxide) electrodes in 1M H₂SO₄ electrolyte were compared with TiO₂ electrodes and the other electrodes are GaP electrodes in both cells, as shown in Table 4.2.1b.

Table 4.2.1b Efficiency of self driven hydrogen cells

Electrode couple	I ($\mu\text{A}/\text{cm}^2$)	Total power ^{***} ($\mu\text{W}/\text{cm}^2$)	η_5 (%) in xenon light [*]	η_5 (%) in Sunlight ^{**}
$\text{LaCrO}_3\text{-TiO}_2\text{-GaP}$	240	305	0.6	1.8
$\text{TiO}_2\text{-GaP}$	120	148	0.29	0.22

* Xenon power $50 \text{ mW}/\text{cm}^2$

** Sunlight power $75 \text{ mW}/\text{cm}^2$ for AM 2

*** Chemical power output is $1.23XI$, then η_5 is calculated from Eq.4.1.20.

Problems of this electrodes, it did not seem easy to dope lanthanum chromite satisfactorily so that it was thought better to attempt to obtain a mixture of lanthanum chromite with the original photoactive anode. Further work will be carried out to characterize the oxide, study its long-term stability, the optimization for absorption, etc.

A new present form of TiO_2 crystal is a semiconductor/redox electrolyte/semiconductor junction (SES) as photoanode. Nakato et al. (1982)⁽⁷¹⁾ have designed a SES electrode for water photoelectrolysis in photocell without external bias. The structure of the SES is indicated in Figure 4.2.3. It consists of single crystal wafers of n-CdS and n- TiO_2 (0.3-0.7 mm thick) separated by ~ 0.2 mm by an aqueous solution containing 1M NaOH, 1M Na_2S and 1.5 gram atom l^{-1} S which dissolves in a concentrated sulphide solution.

As shown Figure 4.2.4 the onset potential of the anodic photocurrent of the SES electrode in a 1.0 M NaOH aqueous solution lies in a much more negative region than that of an n- TiO_2 electrode. This means that water can be photodecomposed efficiently by a photocell equipped with a SES photoanode, a platinum counter electrode and a 1.0 M NaOH aqueous solution. Considerable gas evolution was observed at both electrodes,

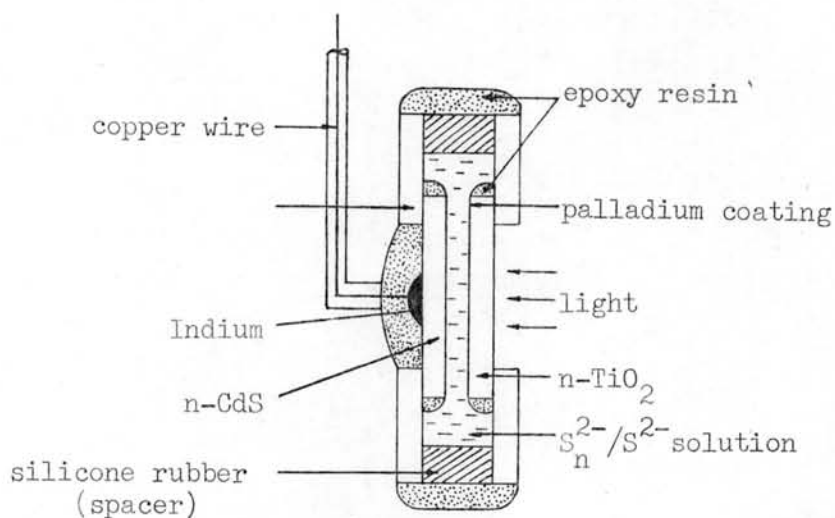


Figure 4.2.3 Schematic diagram of an $n\text{-CdS-Sn}^{2-}/\text{S}^{2-}$ solution- $n\text{-TiO}_2$ junction (SES) electrode. ⁽⁷¹⁾

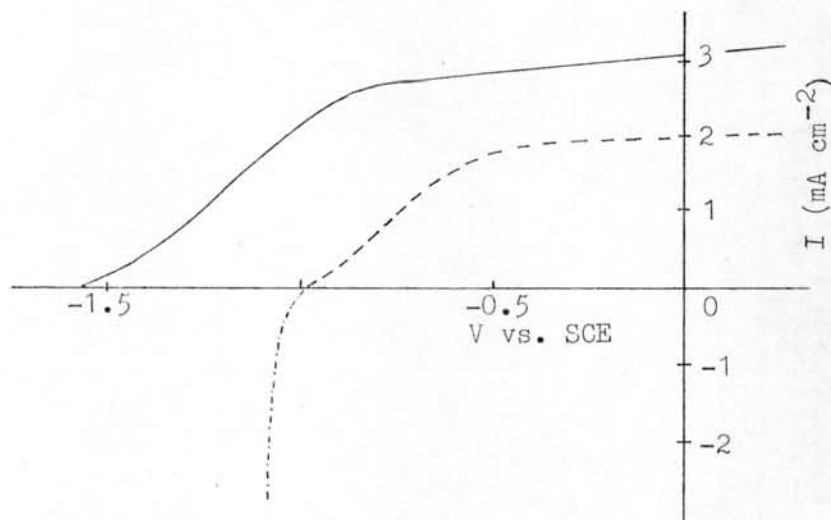


Figure 4.2.4 Current-potential curves for the SCE (—) and $n\text{-TiO}_2$ (---) electrodes under illumination and that for a Pt electrode (· · ·) in a 1.0 M NaOH aqueous solution. Illumination intensity for the $n\text{-TiO}_2$ electrode is about one-eighth of that for the SES. ⁽⁷¹⁾

but they did not collect gases, then there are no conversion efficiency calculations in this paper. They have found that the current was also generated with two monochromatic light beams, one in the range <410 nm and the other in the range 450–520 nm, but not with either of them alone. These results suggest that the current flows only if both n-TiO₂ and n-CdS are excited. The light in the range of 410–450 nm seems to be absorbed mostly by the sulphide-polysulphide solution. The above results can be explained by an energy level diagram for the photocell, as shown in Figure 4.2.5.

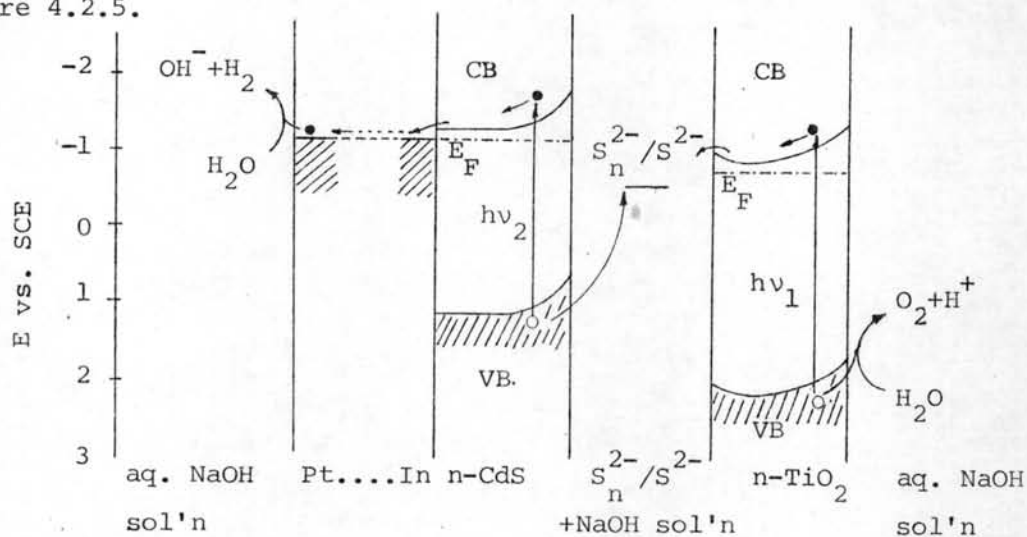


Figure 4.2.5 An energy level diagram for a photocell made of SES and Pt electrodes.⁽⁷¹⁾

Because the inner sulphide-polysulphide solution and the solution outside the SES electrode have nearly the same pH (~14), the energies of the conduction band edges of n-TiO₂ in the dark at both inner and outer surfaces must be equal. However, the accumulation of positive charges in the sulphide-polysulphide solution by injection of holes from the n-CdS under illumination will press down the conduction band energy at the inner

surface of n-TiO₂. A stationary state will be attained by balancing the hole injection from n-CdS with the electron injection from n-TiO₂. The electrons are excited twice in the SES, reaching a level high enough to reduce water at the counter platinum electrode.

The present SES electrode is an interesting structure for a semiconductor with small bandgap (e.g. CdS, CdSe etc.) to be used more desirably for efficient utilization, especially water decomposition.

4.2.2 Thin Film Titanium Dioxide Electrodes

For practical photocell applications, low cost polycrystalline electrode materials will probably be required for large area electrodes. The polycrystalline thin film of TiO₂ formed on a titanium base is more interesting than polycrystalline formed by pressing TiO₂ powder into disks and sintered at high temperature for several hours.

For the first time (1975), Fujishima et al.⁽³³⁾ studied many methods of forming oxide films on metal, such as electrochemical formation, thermal formation of oxide films in a electric furnace and by simple heating. TiO₂ thin films formed on titanium metals by heating in the flame of a Bunsen burner at 1300-1350°C, they showed good photoelectrochemical behavior, the photocurrents on these oxide electrodes were nearly as large as those obtained with the single crystal rutile electrode (Figure 4.2.6). Thickness of the formed oxide film seemed greater than those formed by electrochemical oxidation or thermal oxidation in the electric furnace. Experimental results are discussed in 2.2.1. However, hydrogen synthesis by water photoelectrolysis under sunlight in this photocell also required pH bias. Recently, TiO₂ thin by simple heating at 500°C has be used on photocells

without pH bias by Ahlgren.⁽¹⁾ He must bias the photocells with external power for water electrolysis. This paper showed the theoretical analysis of I-V characteristic for optimization the maximum bias voltage and electrode efficiency. For the TiO_2 electrode, the maximum voltage is about 0.9V and the maximum electrode efficiency is 0.02 %.

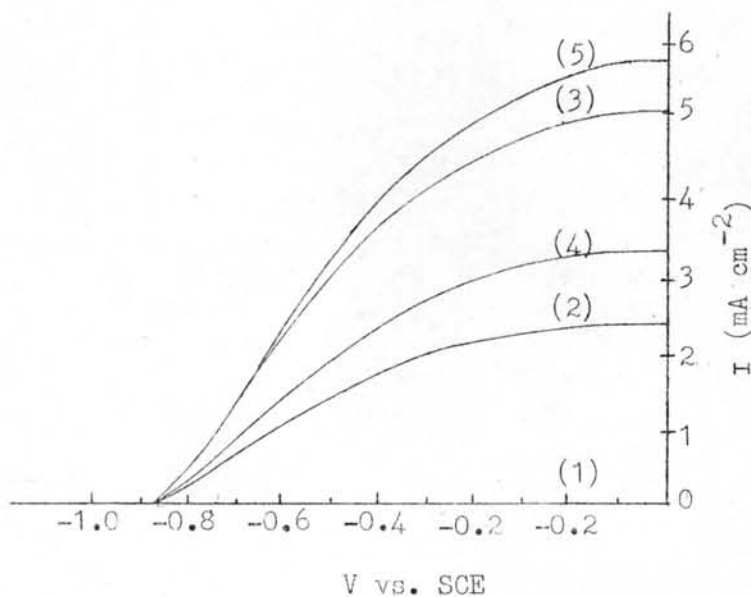


Figure 4.2.6 The I-V characteristics of TiO_2 thin film under irradiation in relation to temperature of heating of 5 min. (1) Ti metal, (2) 1200°C (3) 1300°C (4) 1400°C , (5) rutile single crystal.⁽³³⁾

Chemical vapour deposition can be used in a preparation of thin film, TiO_2 on titanium metal. Hardee and Bard⁽⁴⁴⁾ prepared TiO_2 electrodes using this method and compared it with single crystal TiO_2 . The photocurrent of thin film was about 4 times less than that of the crysted TiO_2 thin film was insufficiently thick to support a full space charge, necessary for separation of opposite charge carriers.

In 1980, Guruswamy et.al.⁽⁴¹⁾ obtained La_2O_3 in TiO_2 thin film and involved oxides of Cr_2O_3 , Au_2O_3 , Rh_2O_3 and V_2O_3 on a titanium base. This method used for TiO_2 crystal also gives a good photoelectrode (see 4.2.1). The electrodes were made by heating a paste of lanthanum oxide, La_2O_3 , with the individual oxides of Cr_2O_3 , Au_2O_3 , Rh_2O_3 , V_2O_3 on a titanium base. The photocurrent observed was found to be 2-6 times higher than those obtained with a TiO_2 single crystal for the same intensity of the solar spectrum. The absolute efficiency for the based cells of LaCrO_3 , LaAuO_3 , LaRhO_2 and LaVO_3 varies between 5.8 % for the solar spectrum, as compared with about 1.5 % for TiO_2 . However, the preparation of these electrodes is not easy, and the stabilities of electrodes in electrolyte must be investigated further.

In order to decrease the cost of thin film electrodes, glass and also plastic are used as the substrate (or base) of TiO_2 .⁽⁴³⁾ Fleischauer and Allen⁽²⁵⁾ used Sn-doped In_2O_3 on glass for the base of a TiO_2 electrode by radio-frequency sputtering. An applied bias voltage ($\geq 0.2\text{V}$) was necessary for visual observation of sensitized hydrogen formation on the cathode under illumination of 400-500 nm wavelength. By the same reactive sputtering, a Ti-metal was used the base of TiO_2 electrode. Soliman and Seguin(1981)⁽⁸⁹⁾ deposited TiO_2 film on heated glass substrates and formed n^+/n layered structure for this electrode (Figure 4.2.7)

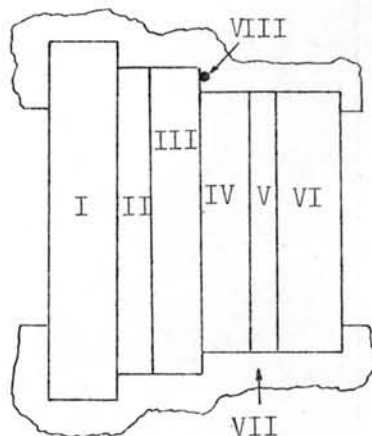


Figure 4.2.7 Electrode configuration: I, glass substrate, II titanium film III. gold layer, IV titanium, V, diffusion region (n^+), VI n-Type semiconductor, VII epoxy, VIII copper wire.

The n^+ is defined as the more doped concentration region. The titanium layer (II) provides strong adherence between the gold layer and the glass substrate. The gold layer (III) provides electrical contact to the external circuit. The layer of titanium (IV) is an ohmic contact region to the semiconductor. The n^+/n layer provides the TiO_2 thin film to expose the light. This region opposes the hole diffusion of holes from the n-layer to n^+ -layer, while favoring the transport of electrons. However, this electrodes was not good enough for use in photocell, the response wavelength was the short range of 280-310 nm.

4.3 Semiconductor Electrode Development for Sunlight Response

4.3.1 Small band gap semiconductor

Many semiconductors with small band gaps are unstable in aqueous electrolyte under illumination (e.g. some semiconductors in Table 3.4.8), except p-GaP electrode⁽⁹²⁾, in which the photocell could give the

maximum efficiency 0.1 % (by Eq.4.1.18 for η_3) with an external bias of 1.3 volts. However, there are some of these, such as CdS which can be stabilized in ferri-ferrocyanide-solution⁽¹⁰⁾, but then no water photolysis result. The task of investigating suitable electrolytes for these semiconductors has been recently attempted. Fan⁽²³⁾ has demonstrated the hydrogen evolution on p.GaAs in N,N'-dimethyl-4, 4' - bipyridinium (methylviologen, MV^{2+}) solution. This system requires catalysts of PtO_2 for hydrogen generation, as shown in Figure 4.3.1. The photoreduction of water directly from this system is slow and inefficient. Recently, Bocarsly⁽⁸⁾ has attempted to use p-type Si in the above electrolyte, but no hydrogen evolution.

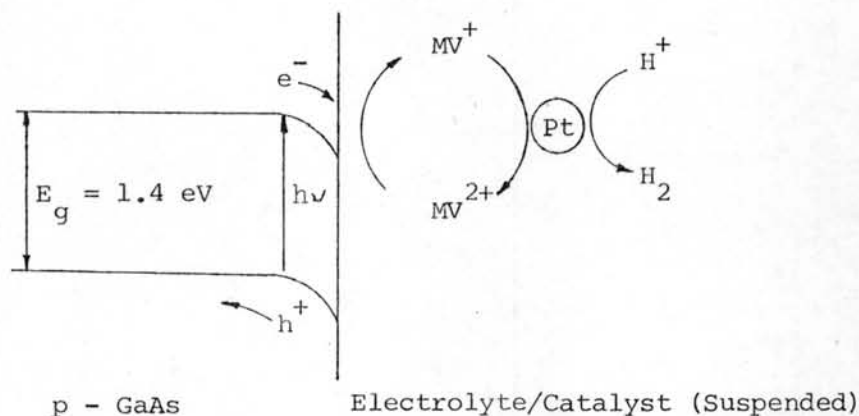


Figure 4.3.1 Representation of hydrogen generation scheme.

The advantage of the attempt would be that semiconductors with small band gaps can be used and therefore a large part of the solar spectrum will be absorbed.

4.3.2 Heterostructure formation

The object of heterostructure formation is to increase, sunlight response of semiconductors with large band gaps (e.g. TiO_2 , SnO_2)

by coating with dye materials, this method is called dye sensitization. Another, small band gap semiconductor with the heterostructure formation can be stabilized in photoelectrochemical cells, by coating these semiconductors with semiconductors with large band gaps.

For dye sensitization the principle structure of electrode is shown in Figure 1.2.2, and for example SnO_2 electrode ($E_g=3.5\text{eV}$), coated with chlorophyll is as photoelectrode for a photovoltaic cell (see 2.4.3). Maruska and Ghosh⁽⁵⁸⁾ coated TiO_2 electrodes with dye (e.g. cyanine, merocyanine) by vacuum deposition and solution dipping. Peak sensitization wavelengths were found in the range of 450-550 nm, in the visible portion of the spectrum. The highest quantum efficiency (Eq.3.5.2d) measured was about 0.7 % at 510 nm with several merocyanine dyes, while a cyanine dye showed a peak sensitization at 550 nm with a quantum efficiency of 0.1 %. They found the problems of this sensitization, the stability of heterojunction and the rapid degradation of response. However, the dye sensitization of photoelectrodes is still not used in PEC'S for hydrogen synthesis.

The other formation, such as depositing TiO_2 on GaAs, GaP, CdS, CdSe and Si, they would be the good photoelectrode for photovoltaic cells, but not able to use for hydrogen production. For the formation of heterojunction, the location of energy band edges of two semiconductors will be considered, there are two possible the heterojunction forms, as Figure 4.3.2a and b. For Figure 4.2.2a illustrates the case where both the small and the wide band gap semiconductors are highly conducting n-typed materials, here a discontinuity in the valence bands is encountered and there is a high barrier to hole flow from the small to the large band gap semiconductor, it is not a good formation For the other, there are not barriers for moving the electrons and holes through the junction.

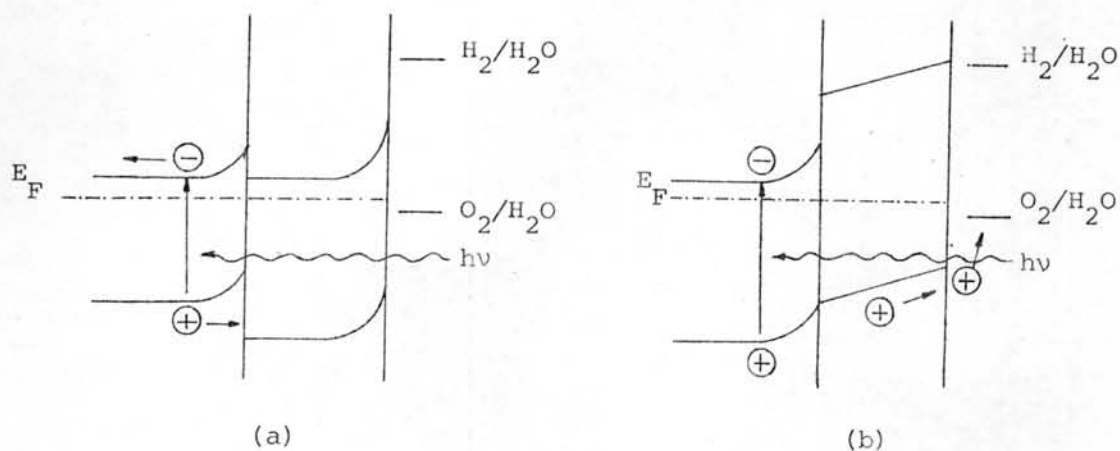


Figure 4.3.2⁽⁶⁰⁾ Energy diagrams for heterojunction electrodes

Studies were also made on structure where a thin film, such as gold,⁽⁶²⁾ was used to protect small band gap semiconductors from corrosion. Of course, a film of metal sharply reduces the light transmission of the substrate. Recently Fu-Tai Lion⁽³⁰⁾ has attempted to build the $\text{Fe}_2\text{O}_3/\text{TiO}_2$ heterojunction electrodes for photoelectrolysis, but not increasing the light response, it is still a response at short wavelength of 300-400 nm. The stability and light transparent of the junction will require further studies.

4.3.3 Impurity sensitization.

For impurity doping in a semiconductor, there are two possible mechanisms of location of impurity atom, one can substitute. The semiconductor atom in the crystal for formation of n-or p-type form ; such as Si is substituted by As or Ga (Figure 3.3) The other, impurity atom cannot substitute the semiconductor atom, but is only located in the crystal. To form of n or p type semiconductors, the impurity atom must has a suitable valence electrons (see 3.1.2) as well as the atomic radius, which is nearly

equal to the substituted semiconductor atomic radius, and concentration of impurity (N_D or N_A) is limited by its solubility in the semiconductor.

Impurity sensitization is used for large bandgap semiconductors such as TiO_2 to visible light response. Salvador⁽⁸²⁾ has doped TiO_2 (Ti-3d²4s² and 1.47 Å of atomic radius) with Nb_2O_5 (Nb-4d⁴5s¹ and 1.46 Å) to form n-type TiO_2 electrode and examined the influence of the doping Nb on the behaviour of n- TiO_2 in water photoelectrolysis. He found that optical absorption coefficient and hole diffusion length were not sensibly influenced by the dopant concentration up to level of about 2 %.

For TiO_2 electrodes for PEC'S, by doping impurities of transition metals (e.g. Cr, Fe, Ni, Zn), the solar response of these electrodes is better than the above method. The transition metals do not substitute Ti atoms of the crystal. The excitation of the impurity into the TiO_2 bands can result in free electron and holes formation. This is described by the following equations and Figure 4.3.3.⁽⁵⁸⁾

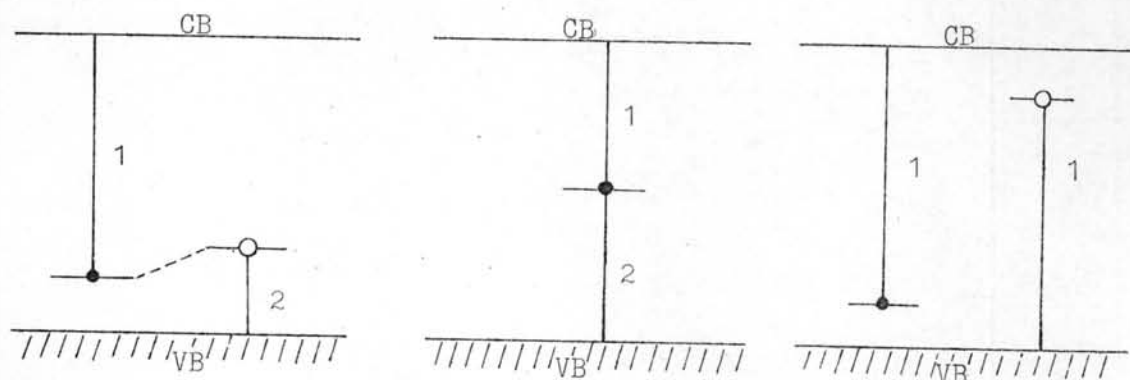
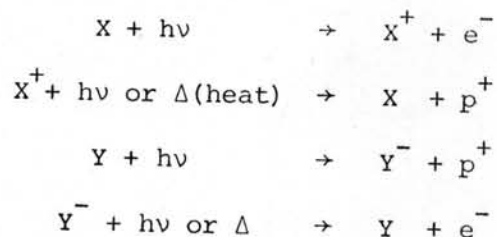


Figure 4.3.3 Possible absorption processes due to dopant impurities in a material such as TiO_2 .

The possible reactions are;



From Figure 4.3.3, (a) shows the electron excited from the impurity level to the conduction band. The ground state level of the ionized impurity level may shift. The hole in the ground state level can be ionized by heat or light and result in a free carrier. Figure 4.3.3(b) is similar to case (a) with the exception that the impurity level is roughly midway between bandgap and it does not shift after ionization. Figure 4.3.3(c) shows the case where the catalyst material is doped with two impurities. Optical excitation in these levels gives rise to free electrons and free holes. Obviously the cases described need roughly two photons for excitation. The photons may be of the same energies or one may be much larger than the other.

Ghosh and Maruska (1977)⁽⁵⁸⁾ demonstrated the doping of TiO_2 electrode with Al, the sunlight conversion efficiency raised to 1.3 % from 0.4 % of undoped TiO_2 in 5M KOH electrolyte, Pt counter electrode, and an external bias were supplied. They showed a good fit of their experimental data with the relationship given in Eq.3.5.1a, and determined the barrier width, l_b and the hole diffusion lengths, l_p . The longer diffusion lengths were found for Al-doped TiO_2 (4.5μ), while both barrier

widths were to 10^{-6} cm (Figure 4.3.4).

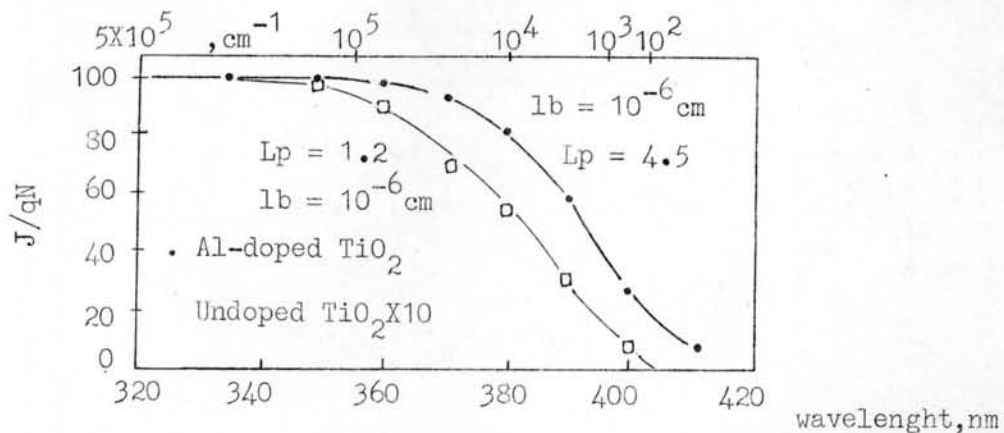


Figure 4.3.4 Best fit of the theoretically derived Schottky barrier response curves to the experimentally determined response of undoped and Al doped TiO_2 devices. (58)

For transition metal doping, the starting substrate forms are single crystal, (36,59) powder (40,82) and Ti metal, two later forms will form TiO_2 polycrystalline during doping preparation. For Ti-metal as substrate, (41,70,61) this electrodes is doped with Ni, Cr and Zn, and the quantum efficiency is not up to 30 %. The others, experimental results is summarized in Table 4.3.3, the wavelength of light is a range of 350-360 nm, and their barrier width are 10^{-5} cm.

Table 4.3.3 The barrier widths and the hole diffusion length in TiO_2 doped with the transition metals. (58,59)

Transition metal dopant	undoped*	Al*	Al	Cr	Cr,Al	Mn	Fe
Diffusion length (μ)	1.6	4.5	8	0.2	0.8	1	2
Quantun efficiency (%) of Eq.3.5.2d	9	80	80	14	45	58	70

* their barrier width are 10^{-6} cm.

However, only single crystal substrate is used in photoelectrode in PEC'S for efficiently hydrogen production, and a good impurity material for TiO_2 electrode is aluminium (Al).

4.4 Photoelectrocatalytic Cells

4.4.1 Semiconductor Catalyst Systems

There are semiconductor materials as particle catalyst in a photoelectrocatalytic cell, such as TiO_2 , ZnO , CdS etc. The photogenerated electrons and holes can be effectively separated in the interface suspended in aqueous or other solution (Figure 1.2.3). The net result of such redox reactions (e.g., H_2 , NH_3 and CH_2OH synthesis) at interface of semiconductor are shown in Figure 4.4.1.

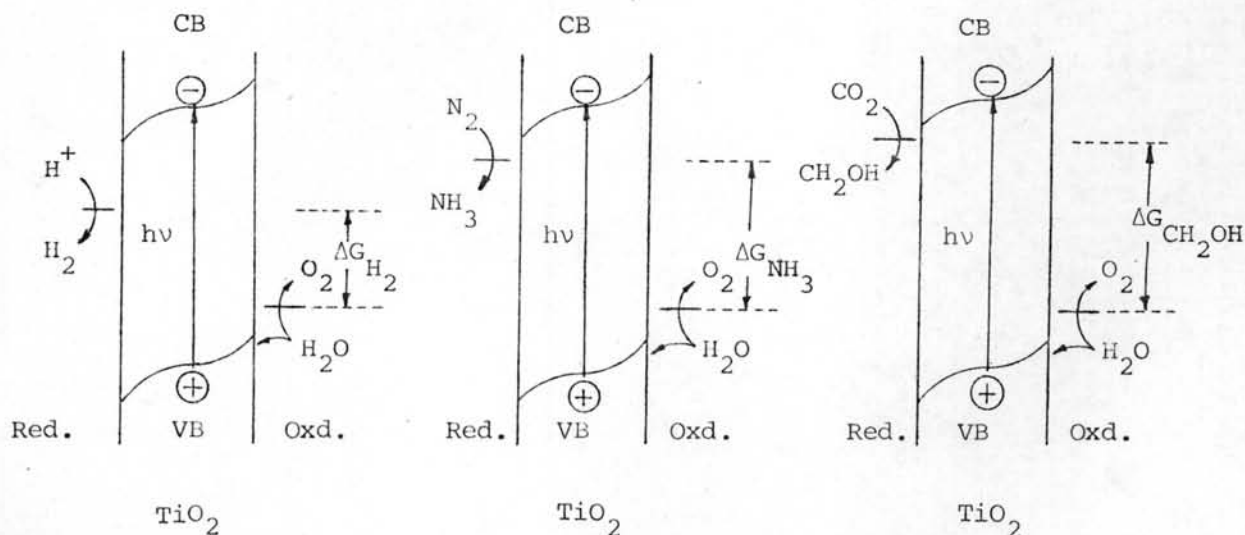


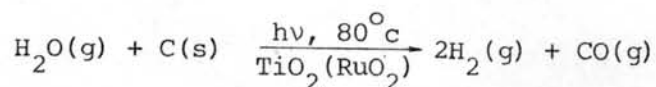
Figure 4.4.1 Schematic presentation of photoelectrocatalytic redox reactions on semiconductors (TiO_2). Red. and Oxd. refer to the reduction and oxidation reactions, respectively (see 3.4.1) and ΔG is the free energy of the products (Table 2.1.3).

In most instances, what one intends to make proceed is the reduction rather than the oxidation, since chemical reduction implies fuel formation.

In this section, a hydrogen synthesis by this cell will be more referred to a useful fuel than the others (NH_3 and CH_2OH , there are some literature surveys of them in 2.2.2 and 2.2.3)

The photoelectrocatalytic cell is a system which duplicates plant photosynthesis, there is the chlorophyll pigment suspended in a chloroplast cell in the leaf. Up to now, the experiments of photoelectrocatalytic cells have been small scale in laboratories, and hydrogen yield will be analyzed by a mass spectrometer.

In the early experiment (1977),⁽²⁷⁾ hydrogen synthesized by this cell, consisted of Fe doped, TiO_2 powder in aqueous solution under illumination by Hg lamp and sunlight. They gave low yields and stopped after a few hours, because the reactor was small, and products (H_2 and O_2) were not separated, then a reversible reaction occurred; $\text{H}_2 + \frac{1}{2}\text{O}_2 \rightarrow \text{H}_2\text{O}$. In 1979, Damme and Hall⁽²⁰⁾ studied this system in a flow system in order to move the reaction products from the catalyst completely. Helium was saturated with H_2O at room temperature and flow over the catalyst was spread uniformly on a quartz optical plate of area 5 cm^2 which made up the bottom of a flask. The TiO_2 could be illuminated from below with white light. They demonstrated this system (the gas-solid interface on catalyst), should be more stable when TiO_2 was immersed in liquid. Also, Kawai and Sakata⁽⁵¹⁾ used solid carbon in photocatalytic hydrogen production on TiO_2 mixing RuO_2 powders from water vapour (the gas-solid interface), then



They found the relative quantum efficiency of H_2 evolution in TiO_2-RuO_2 , C, H_2O system increased at least 10^2 times that from the TiO_2-H_2O system. They⁽⁵²⁾ used TiO_2 mixing RuO_2 powders again in this cell (Figure 4.4.2) without solid carbon. The rate of hydrogen per 100 mg TiO_2-RuO_2 and 20 hours was 0.55μ mole/hr at steady state under lamp irradiation ($\lambda > 320$ nm).

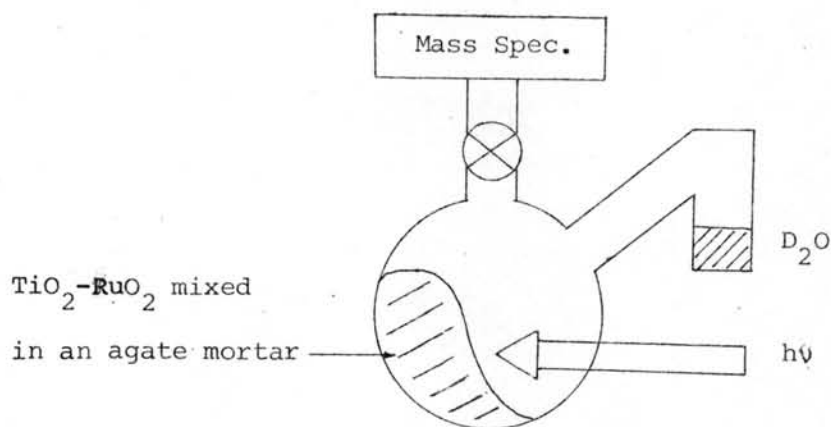


Figure 4.4.2 A scheme of the experiment for photocatalytic hydrogen and oxygen from gaseous water.⁽⁵²⁾

In 1980, $NiO-SrTiO_3$ catalyst was used in this cell by Domen et.al,⁽²²⁾ the hydrogen evolution was steady for more than 100 hours from water vapour, and 0.2μ mole/hr (0.44×10^{-3} ml/hr) and 0.1μ mole of oxygen by gas chromatography.

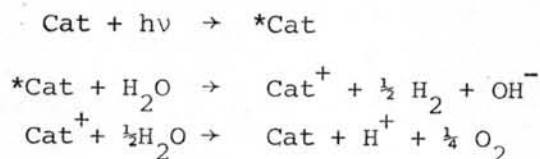
However, the liquid-solid interface (catalyst suspended in water) is still investigated in further studies. Sato and white⁽⁸⁴⁾ used $Pt-TiO_2$ catalysts (platinized powder titanium dioxide catalyst⁽⁵⁵⁾) for photodecomposition of water, then the rate of hydrogen evolution was 0.35μ mole/hr in 180 ml of reactor volume. But, after 2 hours the rate decreased to about 0.1μ mole/hr. In 1981, Kawai and Sabata⁽⁵³⁾ studied $Pt-TiO_2$

catalyst used in decomposing poly-vinylchloride, protein, algae, dead insects and excrement for hydrogen production without the release of halogen or nitrogen compounds in the gas phase under Xe-lamp irradiation. This work may be useful for the production of hydrogen fuel from many organic resources and waste materials in the future.

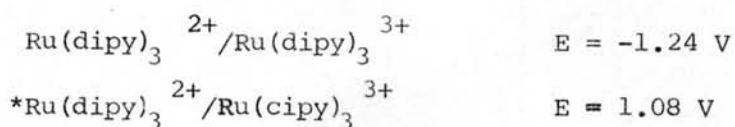
The other catalyst, CdS is stable in cysteine and ethylenediaminetetraacetic acid (EDTA) solution, therefore hydrogen production by photocatalysis of water in suspensions of CdS particles in the above solution has been demonstrated by Darwent (1981).⁽²¹⁾ However, the stability of CdS catalyst is still an important problem.

4.4.2 Complex Compound Catalyst Systems

Complex compounds in aqueous solution can absorb the light energy in the visible range and lead to the dissociation of water molecules. The hypothetical formulations of water photodecomposition was demonstrated by Balzani et al.⁽⁴⁾ A general formulation of hydrogen molecules is the redox reaction as follows.⁽¹¹⁾



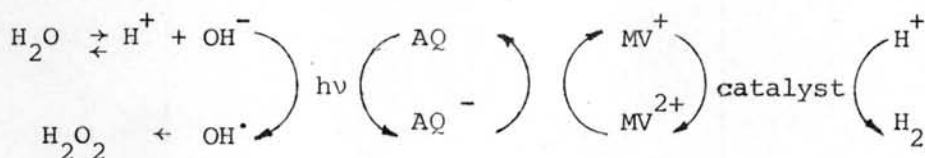
These compounds, in fact, are suitable components of redox systems to be used for solar energy conversion, since they are coloured and can undergo redox reactions without change in their stoichiometry. For example $\text{Ru}(\text{dipy})_3^{2+}$, a ruthenium complex (byp = 2,2 bipyridine), the following values have been obtained for the oxidation potentials of the ground state and the lowest energy excited state:⁽¹¹⁾



This means that the different potential between ground and excited stated is about 2.12 volts, which may be converted into free energy with high efficiency. Giro et.al.⁽³⁷⁾ demonstrated hydrogen synthesis by irradiating with visible light aqueous hydrochloridic solutions of $[\text{Ru}(\text{bpy})_3]^{2+}$ and trivalent titanium, $[\text{Ti}(\text{H}_2\text{O})_6]^{3+}$. Increasing the quantum efficiency and hydrogen yield, dimethyl viologen (MV^{2+}) and Pt particles were added in solution containing $\text{Ru}(\text{bpy})_3^{2+}$ by Kiwi and Cratzel⁽⁵⁴⁾. However, the Ru complex is a photocatalyst but the quantum and hydrogen yields are very low.

The other complex, dinuclear rhodium (I) complex, $[\text{Rh}_2(\text{bridge})_4]^{2+}$ (bridge = 1, 3-diisocyanopropane) is a photocatalyst for hydrogen synthesis in acidic aqueous solution.^(57,67) Mann et al.⁽⁵⁷⁾ found hydrogen evolution by 546 nm irradiation of the Rh complex in HCl solution and the quantum yield was about 0.4%.

In 1980, Okura and Kim-Thuan⁽⁷⁷⁾ attempted to use anthraquinone as a photosensitizer, methyl viologen as an electron transfer agent and colloidal platinum as a catalyst for water splitting into hydrogen and peroxide, as follows;



From the above result, hydrogen evolution was observed in both cases after 40 hours irradiation, it was about 0.13 μmole . Also, they

added haematoporphyrin and hydrogenase in the methyl viologen (MV^+) solution was irradiated by visible light, and hydrogen evolution was observed, the maximum rate was about $6 \mu\text{mole/hr}^{(78)}$. The stability was not demonstrated.

However, the hydrogen production by photoelectrocatalytic cells need much more development in the area of catalysts and solutions for the systems.